Classical Trajectory Study of the Reaction between H and HCO†

Jürgen Troe*,‡ and Vladimir Ushakov‡,§

Institute of Physical Chemistry, University of Göttingen, Tammannstrasse 6, D-37077 Göttingen, Germany, and Institute of Problems of Chemical Physics, Russian Academy of Sciences, 142432 Chernogolovka, Russia

Received: November 9, 2006; In Final Form: December 14, 2006

The thermal reaction between H and HCO was studied by classical trajectory calculations on an ab initio potential. The formation of H_2 + CO, the exchange of hydrogen atoms, and nonreactive encounters, proceeding either via direct or via complex-forming pathways, were separated. The reaction H + HCO → H_2 + CO, with direct and complex-forming components, was found to have a low-pressure rate coefficient of 2.0-($\pm$0.15) × 10^{-10} cm^3 molecule^{-1} s^{-1}, being nearly independent of temperature between 200 and 1000 K. This value is in agreement with the recent experimental value of 1.83($\pm$0.4) × 10^{-10} cm^3 molecule^{-1} s^{-1}. Thermal lifetime distributions of H_2CO* complexes formed in the reaction are only weakly temperature dependent due to a compensation of energy and angular momentum effects.

Introduction

Formaldehyde is an intermediate of the oxidation of hydrocarbons, and its high-temperature reactions have attracted considerable attention (see, e.g., refs 1−6). Within the oxidation mechanism, the pyrolysis of formaldehyde plays an important role such as quantified, e.g., in ref 2. Except at very low concentrations, it is known to proceed via a chain reaction which is initiated by the dissociation

$$H_2CO\ (+M) \rightarrow H + HCO\ (+M) \qquad (1a)$$

in competition with the elimination reaction

$$H_2CO\ (+M) \rightarrow H_2 + CO\ (+M) \qquad (1b)$$

The short chain

$$H + H_2CO \rightarrow H_2 + HCO \qquad (2)$$

$$HCO\ (+M) \rightarrow H + CO\ (+M) \qquad (3)$$

finally is terminated by the reaction

$$H + HCO \rightarrow H_2 + CO \qquad (4)$$

This work focuses attention on reaction 4 and its relation to reactions 1a,b. Reaction 4 has been studied experimentally over the temperature range 300−2500 K, and the results are summarized in Table 1. The data scatter over about a factor of 5, and a value of k_4 = 1.5 × 10^{-10} cm^3 molecule^{-1} s^{-1} over the range 300−2500 K, with an uncertainty of $\pm\Delta$ log k_4 = 0.3, was recommended in the evaluation of ref 6. The most recent value of k_4 = 1.83($\pm$0.4) × 10^{-10} cm^3 molecule^{-1} s^{-1} over the range 295−820 K from ref 7 probably is the most reliable, because the most advanced experimental techniques were employed in its determination.

TABLE 1: Low-Pressure Rate Coefficients k_4

T/K	k_4/10^{-10} cm^3 molecule^{-1} s^{-1}	origin[a]	ref
295−820	1.83($\pm$0.4)	expt	7
298	2.4($\pm$1.0)	expt	22
298	1.1($\pm$0.3)	expt	23
298	1.4($\pm$0.4)	expt	24
350	1.3($\pm$0.4)	expt	24
418	0.96($\pm$0.3)	expt	24
1200−1900	3.6($\pm$1.8)	expt	25
285	5.5($\pm$3)	expt	26
1800−2700	3.3($\pm$2)	expt	27
298	4.0($\pm$1)	expt (rel)	28
315−490	2.1($\pm$0.3)	expt (rel)	29
200−1000	2.0($\pm$0.15)	theor (CT)	this work
300−1000	0.95	theor[b] (VTST)	8
1100	1.0	theor[b] (VTST)	8
2000	1.3	theor[b] (VTST)	8
3000	1.7	theor[b] (VTST)	8

[a] Expt = experiment, rel = relative to O + HCO, and theory. [b] Abstraction + elimination.

The considered reaction 4 takes place on the potential energy surface of formaldehyde and, therefore, should be discussed in relation to reactions 1a,b. A first approach in this direction was undertaken by Harding and Wagner,[8] who concluded that reaction 4 mostly occurs via hydrogen abstraction rather than via formation of H_2CO with subsequent elimination (eq 1b). Pressure dependences, due to a chemical activation mechanism with the possibility of collisionally stabilizing H_2CO, were predicted not to be important up to several bar of gas pressure. The treatment of ref 8 employed an ab initio potential together with variational transition state theory (VTST) and RRKM calculations. The recent more elaborate work on the potential and its analytical representation[9] calls for an extension of Harding's and Wagner's calculations of k_4. The complicated dynamics on the H_2CO potential, such as identified in recent years,[10] suggests that treatments using VTST and simple RRKM theory have to be modified. It is the aim of this work to proceed in this direction and to provide a new theoretical calculation of k_4, analyzing its various components on the basis of the now available information.

This study should be seen in connection with recent classical trajectory (CT) calculations,[10] on the ab initio potential from

† Part of the special issue "M. C. Lin Festschrift".

* Corresponding author. E-mail: shoff@gwdg.de.
‡ University of Göttingen.
§ Russian Academy of Sciences.

10.1021/jp0674017 CCC: $37.00
Published on Web 01/26/2007

ref 9, of the branching ratio between channels (1a) and (1b), with SACM (statistical adiabatic channel model)/CT calculations of the absolute values of thermal and specific rate constants for channels (1a) and (1b) from ref 11 and with the theoretical analysis of experimental dissociation rate coefficients[12,13] and photolysis quantum yields.[14] CT calculations on the ab initio potential from ref 9 are performed and analyzed with respect to all pathways of the reaction. There is the major contribution from the direct abstraction process

$$H + HCO \rightarrow H_2 + CO \qquad (4a)$$

but some formation of H_2 + CO also proceeds via H_2CO-complex formation

$$H + HCO \rightarrow H_2CO^* \rightarrow H_2 + CO \qquad (4b)$$

This work also allows one to identify atom exchange processes of the type

$$H_a + H_bCO \rightarrow H_aH_bCO^* \rightarrow H_b + H_aCO \qquad (4c)$$

competing with direct exchange

$$H_a + H_bCO \rightarrow H_b + H_aCO \qquad (4d)$$

Finally there are nonreactive processes which either proceed directly,

$$H_a + H_bCO \rightarrow H_a + H_bCO \qquad (4e)$$

or after complex formation

$$H_a + H_bCO \rightarrow H_aH_bCO^* \rightarrow H_a + H_bCO \qquad (4f)$$

The reliability of the theoretical calculations is believed to be now of the same order as that of the best experimental values such that the quality of the data can be validated. The absence of a temperature dependence of k_4 is confirmed, the approximate ratio k_{4b}:$k_{4a} \approx$ 1:1.3 (at 500 K) from ref 8 is determined more accurately, and the pressures effects on k_4 are discussed.

Calculational Method

The present calculations were done on the ab initio potential of H_2CO in the electronic ground state from ref 9 and its analytical representation from refs 10 and 15. Classical trajectories (CT) on this potential were calculated starting from H + HCO with center-of-mass (com) distances of 20 Å. Details of the CT calculations were described in our series of SACM/CT studies published previously; see, e.g., refs 16−18. To achieve statistical errors of 1%, about 10^5 trajectories were run for each individual result, i.e., for each rate constant at each temperature. In this work initial conditions were sampled randomly from thermal distributions which were classical for translations and rotations but quantum for the vibrations of HCO. A temperature range 200−1000 K was covered. Higher temperatures, because of uncertainties in the potential, were not considered. The vibrational zeropoint energy problem of CTs in our work was handled as described in ref 18; i.e., all trajectories were rejected which finally lead to products with vibrational energy below their respective zeropoint energies. However, their contribution was accounted for by a prorata increase of the results for nonrejected trajectories. It should be emphasized that this problem was of only marginal importance in this study.

The CT calculations led to thermal cross sections and probabilities for the various competing processes which then were converted to rate coefficients such as described in ref 16. The processes resulting from H + HCO encounters were identified in the following way. There was a clear distinction between trajectories which spent short (less than 0.1 ps) or much longer times at com distances smaller than about 2.5 Å. The former group was termed "direct", and the latter, "complex-forming". Equivalently the potential energy was tracked along each trajectory; complex-forming encounters then were identified by their exploring of configurations with small potential energy. All trajectories were followed from the beginning to the final separation of the products such that nonreactive processes, atom exchange, and H_2 formation could clearly be separated.

While direct encounters were characterized by lifetimes of less than 0.1 ps, complex-forming encounters had thermally averaged lifetimes of about 5 ps. We determined lifetime distributions for various temperatures such as illustrated in the next section. We emphasize, however, that CT calculations, because of their classical nature, do not lead to correct values of the lifetimes. Instead, the classical results in a suitable way have to be combined with quantum-statistical rate theory, e.g., within SACM/CT treatments such as elaborated in the forthcoming publication.[11] In this work, therefore, only qualitative conclusions are drawn from the derived classical lifetime

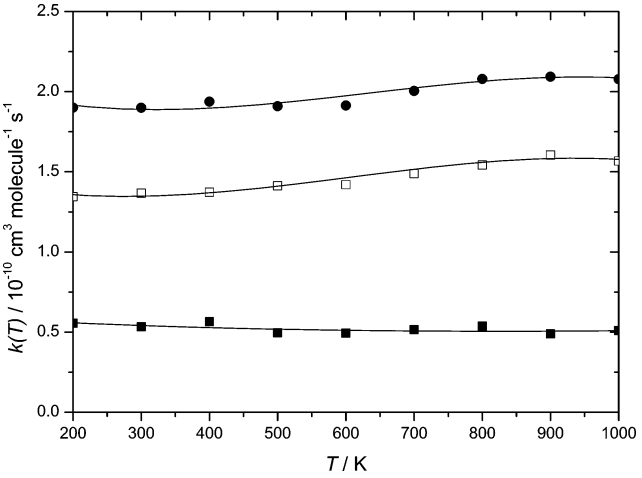

Figure 1. Low-pressure rate coefficients $k_4 = k_{4a} + k_{4b}$ (●) for the reaction H + HCO → H_2 + CO via direct processes (k_{4a}, □) and complex formation (k_{4b}, ■).

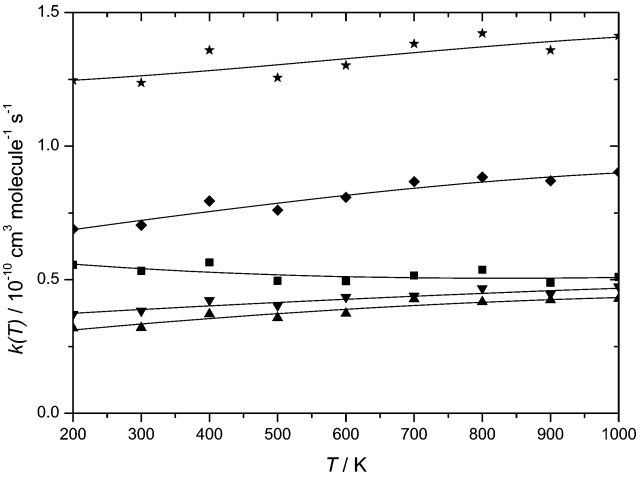

Figure 2. Low-pressure rate coefficients of encounters H + HCO proceeding through complex formation and leading to the formation of H_2 + CO (k_{4b}, ■), atom exchange (k_{4c}, ▲), and nonreactive encounters (k_{4f}, ▼). Sums: $k_{4c} + k_{4f}$ (◆); $k_{4b} + k_{4c} + k_{4f}$ (★).

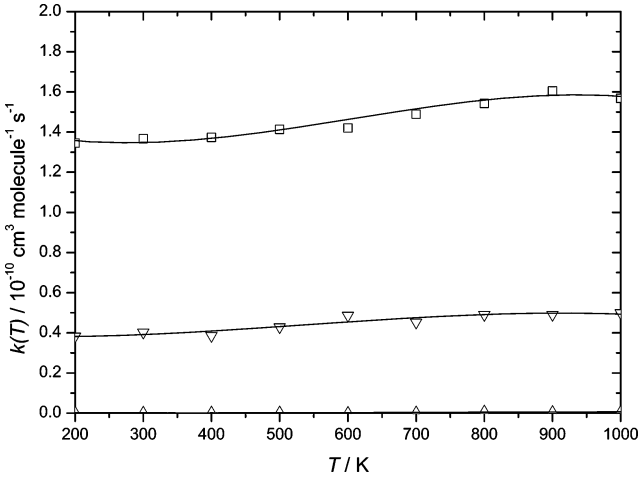

Figure 3. Rate coefficients of encounters H + HCO proceeding via direct processes and leading to the formation of H_2 + CO (k_{4a}, □), atom exchange (k_d, △), and nonreactive encounters (k_{4e}, ▽).

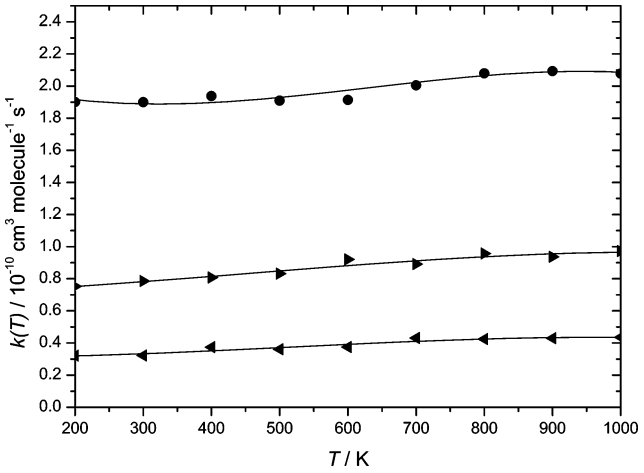

Figure 4. Low-pressure rate coefficients for H + HCO → H_2 + CO (k_{4a} + k_{4b}, ●), H_a + H_bCO → H_b + H_aCO (k_{4c} + k_{4d}, right-pointing solid triangle), and H_a + H_bCO → H_a + H_bCO (k_{4e} + k_{4f}, left-pointing solid triangle).

distributions. In contrast to the lifetimes, the rate coefficients are probably only slightly influenced by performing CT calculations since the zeropoint energy problem has been handled such as described above.

Results

The results of our CT calculations of thermal rate coefficients are illustrated in the following section. Figure 1 shows the temperature dependence of k_{4a} and k_{4b} as well as of the sum $k_4 = k_{4a} + k_{4b}$ which characterizes the low-pressure rate coefficient of reaction 4. Over the considered temperature range 200−1000 K there is hardly any temperature dependence and a value of

$$k_4 = 2.0(\pm 0.15) \times 10^{-10}\ \mathrm{cm^3\ molecule^{-1}\ s^{-1}} \qquad (5)$$

is determined with a ratio k_{4a}:$k_{4b} \approx$ 3:1. Our value agrees well with the most recent experimental value of $1.83(\pm 0.4) \times 10^{-10}$ cm^3 $molecule^{-1}$ s^{-1} from ref 7 but is about a factor of 2 larger than the low-pressure value of k_4 from ref 8. At the same time a larger abstraction/elimination ratio k_{4a}:k_{4b} is obtained than derived in ref 8. The sources of the differences of the present results and ref 8 are probably multiple, partly being due to an improved potential and partly to the use of CT instead of VTST calculations.

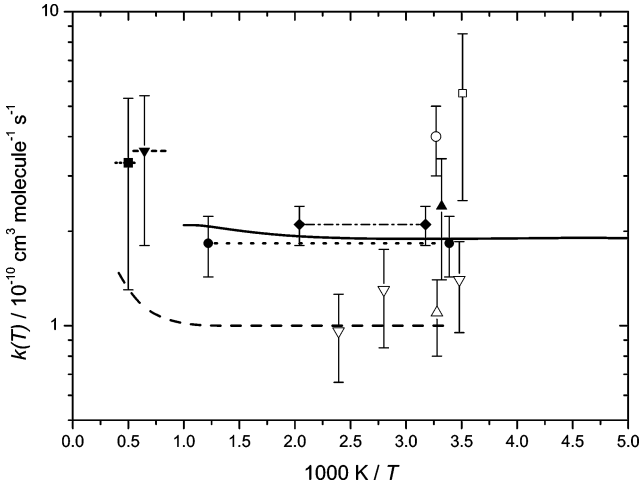

Figure 5. Low-pressure rate coefficients k_4 (theoretical values from CT calculations of this work (—) and VTST calculations from ref 8 (- - -). Experimental values are from ref 7 (•••, ●), ref 22 (▲), ref 23 (△), ref 24 (▽), ref 25 (▼), ref 26 (□), ref 27 (■), ref 28 (○), and ref 29 (− • −, ◆); see Table 1. The relative rate measurements from refs 28 and 29 were calibrated with k(O + HCO) = 1.0×10^{-10} cm^3 $molecule^{-1}$ s^{-1} from ref 6.

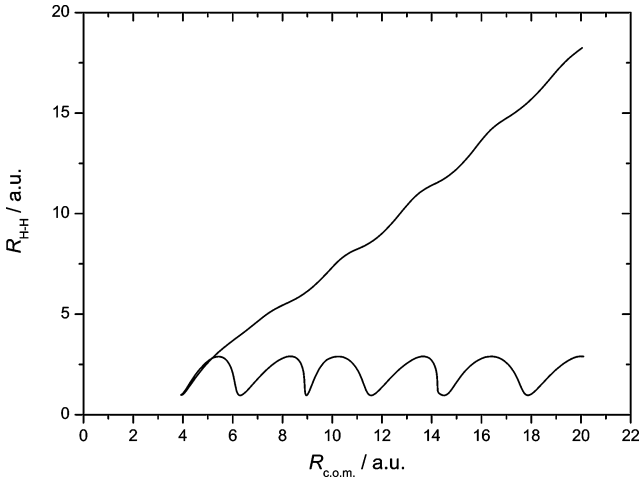

Figure 6. Example of a direct trajectory H + HCO (upper right) → H_2 + CO (lower right).

Figure 2 summarizes low-pressure thermal rate coefficients of all processes which proceed through the formation of long-lived H_2CO*, i.e. values of k_{4b}, k_{4c}, and k_{4f}. This includes processes leading to H_2 + CO, to atom exchange, and to redissociation without atom exchange. The temperature coefficients again are minor, but they are not negligible. In the presence of collisions, a complicated chemical activation situation arises where part of the complexes are collisionally stabilized and part dissociate to H_2 + CO or H + HCO. At infinite pressure, all of the processes (4b), (4c), and (4f) will lead to collisional stabilization of H_2CO and only direct formation of H_2 + CO via reaction 4a will contribute to k_4. We, therefore, expect a decrease of k_4 from the low-pressure value of $k_4 = k_{4a} + k_{4b}$ to $k_4 = k_{4a}$ at infinite pressure. Whether a temporary increase of k_4 at intermediate pressures, due to additional contributions from the complex-forming processes (4c) and (4f), is to be expected would require a more detailed analysis involving a master equation treatment and the use of specific rate constants $k(E, J)$ for H + HCO and H_2 + CO formation from H_2CO*. This treatment is beyond the scope of this work.

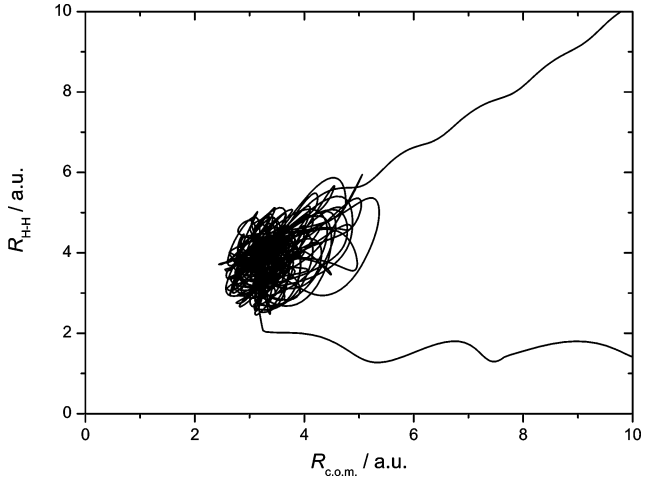

Figure 7. Example of a complex-forming trajectory H + HCO (upper right) → H_2 + CO (lower right).

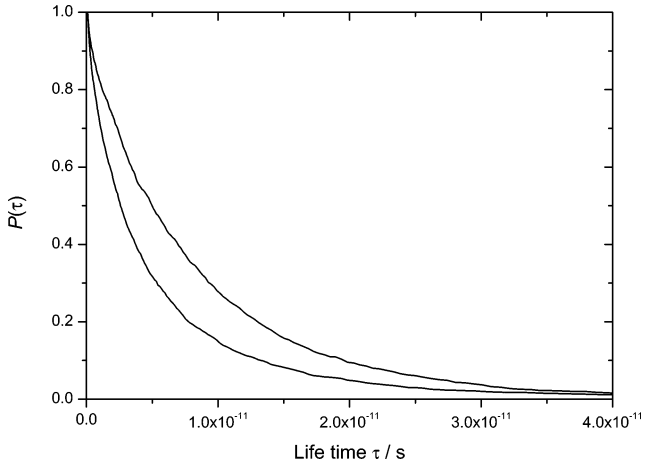

Figure 8. Thermally averaged lifetime distributions of H_2CO^* at 200 (upper curve) and 1000 K (lower curve) from CT calculations. (Quantum lifetimes are longer; see text.)

While Figure 2 illustrated complex-forming components of the reaction, Figure 3 characterizes direct components. One observes that there is practically no direct exchange (eq 4d). Instead, the direct processes are dominated by direct abstraction (eq 4a). About 20% of all direct processes lead to atom exchange (eq 4c). Figure 4 gives total low-pressure rate coefficients for H_2 + CO formation ($k_{4a} + k_{4b}$), H atom exchange ($k_{4c} + k_{4d}$), and nonreactive processes ($k_{4e} + k_{4f}$).

Figure 5 compares the low-pressure rate coefficients for H_2 + CO formation with experimental values such as given in Table 1. The most recent and most sensitive measurements from ref 7 agree well with the present results. The considerable deviations both toward smaller and larger values from earlier studies mostly must be attributed to the difficulties in unraveling the chain mechanism with an incomplete understanding of the primary processes (1a) and (1b).

The CT calculations provide valuable insight into the dynamics of direct and complex-forming encounters. Figures 6 and 7 show two examples for H_2 + CO formation via the two pathways which illustrate that the processes (4a) and (4b) can well be distinguished. Considering only the group of complex-forming encounters, we analyzed the distribution $P(\tau)$ of trajectories spending times longer than τ in the complexes characterized by $R_{com} < 6$ au. Thermally averaged distributions of these lifetimes are illustrated in Figure 8. At first sight, the only small temperature dependence of the average lifetimes appears surprising. However, a more thorough analysis provides the explanation: while the lifetimes decrease with increasing energy, they increase with increasing overall angular momentum of the complexes[11,19] such that the two trends partly compensate. One should note, however, that the CT calculations of lifetimes because of their classical nature provide incorrect absolute values. This statement corresponds to the well-known differences between classical Kassel theory and quantum RRKM theory of unimolecular reactions. More correct lifetime calculations, therefore, require an SACM/CT calculations of the specific rate constants $k(E, J)$ such as given in refs 11 and 19, in combination with CT calculations of branching ratios for H + HCO vs H_2 + CO formation such as described in refs 10, 13, and 14. Thermal averaging of the corresponding results then leads to lifetime distributions which are distributed around approximately 10 times longer average lifetimes than shown in Figure 8. It is not the aim of this study to inspect the pressure dependence of k_4 when reaction 4 under high-pressure conditions becomes of chemical activation nature. This treatment requires a thorough account of the relevant $k(E, J)$ and collisional energy transfer properties which appears premature at this stage. However, the fact that specific rate constants[11,19] above threshold soon exceed 10^{10} s^{-1} indicates that k_4 should remain close to its low-pressure value up to gas pressures of several bar. This is confirmed by the absence of the observation of a pressure dependence in the measurements of k_4 from Table 1. Similar conclusions were drawn in the preliminary treatment of ref 8.

Conclusions

The present classical trajectory calculations of H + HCO encounters allowed us to distinguish reactive and nonreactive processes. Thermal rate coefficients for formation of H_2 + CO, in the low-pressure range of the reaction, between 200 and 1000 K were found to be nearly temperature independent and equal to

$$k_4 = 2.0(\pm 0.15) \times 10^{-10}\ \mathrm{cm^3\ molecule^{-1}\ s^{-1}}$$

This value agrees well with the recent experimental value of $k_4 = 1.83(\pm 0.4) \times 10^{-10}$ cm^3 $molecule^{-1}$ s^{-1} from ref 7. k_4 was shown to have an about 75% contribution from direct and a 25% contribution from complex-forming encounters. Rate coefficients for H atom exchange and for nonreactive encounters were also documented.

The thermally averaged lifetime distributions showed an only weak temperature dependence which is attributed to compensating effects of the increase of specific rate constants $k(E, J)$ with increasing E and the decrease with increasing J (at constant E). The absolute values of the average lifetimes from classical trajectory calculations because of quantum effects need to be modified. This can be done by SACM/CT calculations such as elaborated in ref 11. The then derived values of $k(E, J)$ suggest that major pressure dependences of k_4 should not be expected up to gas pressures of several bar.

Besides lifetime distributions, CT calculations also provide information on the energy distributions of H_2 + CO products from H + HCO encounters. Calculations of this type have been performed in ref 20, and the results can be compared with the corresponding distribution from formaldehyde dissociation such as initiated by photoexcitation.[10,21] It will be interesting in the future to study the effects of different initial conditions of the considered trajectories.

Acknowledgment. We enjoyed many illuminating discussions with M. C. Lin on the modeling of reaction rates in the

fields of combustion and atmospheric chemistry. L. B. Harding, J. M. Bowman, and J. Farnum gave us their analytical representation of the H_2CO potential, which is as gratefully acknowledged as most helpful discussions of this work with L. B. Harding. Financial support from the Deutsche Forschungsgemeinschaft (SFB 357 "Molekulare Mechanismen unimolekularer Reaktionen") is also mentioned.

References and Notes

(1) Lewis, B.; von Elbe, G. *Combustion Flames and Explosions of Gases*, 3rd ed.; Academic Press: Orlando, FL, 1987.

(2) Warnatz, J. In *Combustion Chemistry*; Gardiner, W. C., Ed.; Springer-Verlag: New York, 1984.

(3) Lissianski, V. V.; Zamansky, V. M.; Gardiner, W. C. In *Gas Phase Combustion Chemistry*; Gardiner, W. C., Ed.; Springer-Verlag: New York, 2000.

(4) Miller, J. A.; Pilling, M. J.; Troe, J. *Proc. Combust. Inst.* **2005**, *30*, 43.

(5) Smith, G. P.; Golden, D. M.; Frenklach, M.; Moriarty, N. W.; Eiteneer, B.; Goldenberg, M.; Bowman, C. T.; Hanson, R. K.; Song, S.; Gardiner, W. C., Jr.; Lissianski, V. V.; Qin, Z. http://www.me.berkelex.edu/gri_mech/.

(6) Baulch, D. L.; Bowman, C. T.; Cobos, C. J.; Cox, R. A.; Just, Th.; Kerr, J. A.; Pilling, M. J.; Stocker, D.; Troe, J.; Tsang, W.; Walker, R. W.; Warnatz, W. *J. Phys. Chem. Ref. Data* **2005**, *34*, 757.

(7) Friedrichs, G.; Herbon, J. T.; Davidson, D. F.; Hanson, R. K. *Phys. Chem. Chem. Phys.* **2002**, *4*, 5778.

(8) Harding, L. B.; Wagner, A. F. *Proc. Combust. Inst.* **1986**, *21*, 721.

(9) Zhang, X.; Zou, S.; Harding, L. B.; Bowman, J. M. *J. Phys. Chem. A* **2004**, *108*, 8980.

(10) Zhang, X.; Rheinecker, J. L.; Bowman, J. M. *J. Chem. Phys.* **2005**, *122*, 114313.

(11) Troe, J.; Ushakov, V. G. *J. Phys. Chem. A.* To be published.

(12) Troe, J. *J. Phys. Chem. A* **2005**, *109*, 8320.

(13) Troe, J. *J. Phys. Chem. A.* In press.

(14) Troe, J. *J. Phys. Chem. A.* In press.

(15) Farnum, J.; Bowman, J. M. Private communication, 2006.

(16) Maergoiz, A. I.; Nikitin, E. E.; Troe, J.; Ushakov, V. G. *J. Chem. Phys.* **1996**, *105*, 6263, 6270, 6277; **1998**, *108*, 5265, 9987; **2002**, *117*, 4201.

(17) Troe, J.; Ushakov, V. G.; Viggiano, A. A. *Z. Phys. Chem.* **2005**, *219*, 715.

(18) Troe, J.; Ushakov, V. G. *J. Chem. Phys.* **2001**, *115*, 3621.

(19) Troe, J. *J. Phys. Chem.* **1984**, *88*, 4375.

(20) Rheinecker, J. L.; Zhang, X.; Bowman, J. M. *Mol. Phys.* **2005**, *103*, 1067.

(21) Bowman, J. M.; Zhang, X. *Phys. Chem. Chem. Phys.* **2006**, *8*, 321.

(22) Nadtochenko, V. A.; Sarkisov, O. M.; Vedeneev, V. I. *Izv. Akad. Nauk SSSR, Ser. Khim* **1979**, *28*, 651; *Dokl. Akad. Nauk SSSR* **1978**, *243*, 418; **1979**, *244*, 152.

(23) Hochanadel, C. J.; Sworsky, T. J.; Ogren, P. J. *J. Phys. Chem.* **1980**, *84*, 231.

(24) Timonen, R. S.; Ratajczak, E.; Gutman, D. *J. Phys. Chem.* **1987**, *91*, 692.

(25) Hidaka, Y.; Taniguchi, T.; Kamesewa, T.; Masaoka, H.; Inami, K.; Kawano, H. *Int. J. Chem. Kinet.* **1993**, *25*, 305.

(26) Reilly, J. P.; Clark, J. H.; Moore, C. B.; Pimentel, G. C. *J. Chem. Phys.* **1978**, *69*, 4381.

(27) Cribb, P. H.; Dove, J. E.; Yamazaki, S. *Combust. Flame* **1992**, *88*, 169-186.

(28) Mack, G. P. R.; Thrush, B. A. *J. Chem. Soc., Faraday Trans. 1* **1973**, *69*, 208.

(29) Campbell, I. M.; Handy, B. J. *J. Chem. Soc., Faraday Trans 1* **1978**, *74*, 316.